Significance of Rotating Ground Motions on Behavior of Symmetric- and Asymmetric-Plan Structures: Part II. Multi-Story Structures

Erol Kalkan,[a] M.EERI, and Juan C. Reyes[b]

The influence of the ground motion rotation angle on engineering demand parameters (EDPs) is examined in the companion paper based on three-dimensional (3-D) computer models of single-story structures. Further validations are performed here using 3-D models of nine-story buildings that have symmetric and asymmetric layouts subjected to a suite of bi-directional near-fault records with and without apparent velocity-pulses. The linear and nonlinear response-history analyses (RHAs) are used for evaluating the use of fault-normal and fault-parallel (FN/FP) directions and maximum-direction (MD) to rotate ground motions. This study suggests that individual ground motions rotated to MD or FN/FP directions not always provide conservative EDPs in nonlinear range, but often produce larger EDPs than as-recorded motions. In practice, when a suite of ground motions is used, nonlinear RHAs should be performed by rotating them to the MD and FN/FP directions, and maximum response values should be taken from these analyses as design values. [DOI: 10.1193/072012EQS242M]

INTRODUCTION

When response-history analysis (RHA) is used for design validation of building structures, the ASCE/SEI-7 Chapter 16 (ASCE 2010) is used as the industry standard. According to this document, at least two horizontal ground motion components should be considered for 3-D RHA of structures. At sites within 5 km of the active fault that dominates the hazard, each pair of ground motion components should be rotated to the fault-normal and fault-parallel (FN/FP) directions. In addition, ASCE/SEI 7-10 (Chapter 21) defines maximum-direction (MD) ground motion, a revised definition of horizontal ground motions to develop site-specific design (target) spectrum. In some cases, the building codes mandate that a site-specific design spectrum should be used in lieu of a code-based design spectrum based on mapped spectral acceleration values at short period and at 1 s period.

In the companion paper (Reyes and Kalkan 2015), the influence of rotation angle of the ground motion record on several different engineering demand parameters (EDPs) is examined systematically based on 3-D computer models of single-story structures by varying their vibration period and response modification factor (R). This parametric study provides

[a] United States Geological Survey, Menlo Park, California; ekalkan@usgs.gov (corresponding author)
[b] Universidad de los Andes, Bogota, Colombia; jureyes@uniandes.edu.co

important findings on the significance of rotating ground motions to MD and FN/FP directions. These findings are further validated here by examining both linear and nonlinear responses of multi-story buildings modeled in 3-D as recommended by Anagnostopoulos (2010). The selected systems are nine-story buildings having symmetric and asymmetric layouts. The computer models are subjected to an ensemble of bi-directional near-fault ground motions with and without apparent velocity pulses. At the end, this study provides practical recommendations toward the use of MD and FN/FP directions to rotate ground motions for RHA of building structures.

MULTI-STORY STRUCTURES AND COMPUTER MODELS

The symmetric-plan structure is an existing nine-story steel building with ductile frames (Figure 1) designed as an office building in Aliso Viejo, California (33.585 N, 117.729 W) according to 2001 California Building Code (ICBO 2001) for seismic zone 4 and NEHRP site class D. The earthquake forces were determined by linear response spectrum analysis for the code design spectrum reduced by $R = 8.5$. Its typical floor plan is shown in Figure 2a. The lateral load resisting system consists of two perimeter ductile-steel moment frames in the longitudinal and transverse directions with slotted web steel-beam-to-column connections. The building's interior frames are designed to carry the gravity load only. All structural members are standard I-sections, and the typical floors are made-up of 3 in. metal deck with 3-1/4 in. thick lightweight concrete fill. The building facade consists of concrete panels and glass (Figure 1), and there is a heliport on the roof.

The asymmetric-plan building selected (Figure 2b) is a hypothetical steel building with ductile frames designed to be located in Bell, California (33.996 N, 118.162 W), according to the 1985 Uniform Building Code, which allows for significant plan irregularity.

Figure 1. Nine-story symmetric-plan steel-moment frame building in Aliso Viejo, California (looking toward the northwest).

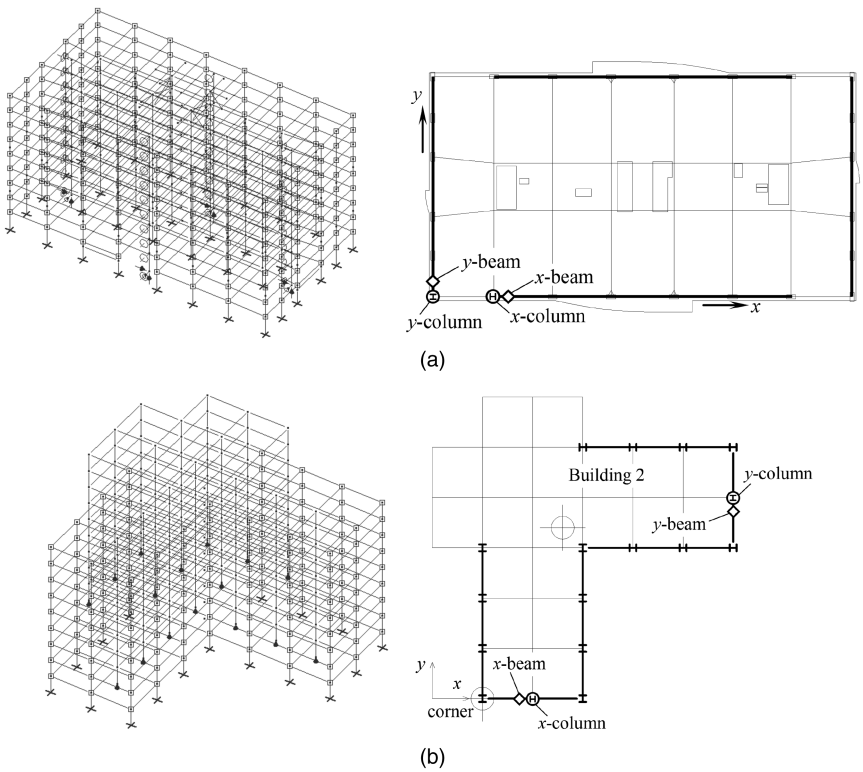

Figure 2. Wire frames for (a) asymmetric-plan building, and (b) asymmetric-plan building; moment resisting frames are shown with thick lines; interior frames are for gravity only.

Both buildings are modeled for dynamic analysis using PERFORM-3D (CSI 2006). The 3-D model of the symmetric building has the following features: (1) Beams and columns are modeled by a linear element with trilinear plastic hinges at the ends of the elements. The bending stiffness of the beams is modified to include the effect of the slab. Axial load-moment interactions in columns are based on plasticity theory. (2) Panel zones are modeled as four rigid links hinged at the corners, with a rotational spring that represents the strength and stiffness of the connection (Krawinkler 1978). (3) The tab connections are modeled using rigid perfectly plastic hinges. (4) The contribution of nonstructural elements is modeled by adding four shear columns located close to the perimeter of the building with their properties obtained from simplified models of the facade and partitions. Nonlinear behavior of these elements is represented using rigid-plastic shear hinges. (5) Ductility capacities of girders, columns, and panel zones are specified according to the ASCE/SEI 41-06 standard (ASCE 2007). (6) Columns of moment-resisting frames and the gravity columns are assumed to be clamped at the base. (7) A standard P-Δ (P = axial force; Δ = lateral deformation) formulation is used to approximate the second-order effects due to nonlinear geometry at large deformations for both moment and gravity frames (Reyes and Chopra 2012).

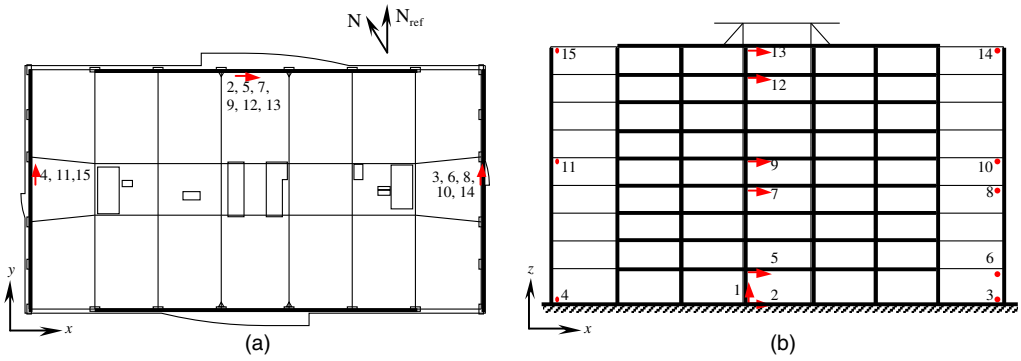

Figure 3. Locations of accelerometers in the nine-story symmetric-plan building: (a) plan view, and (b) south elevation.

The symmetric-plan building was instrumented by 15 accelerometers (Figure 3) by the Strong Motion Instrumentation Program of the California Geological Survey. The 2008 magnitude (M_w) 5.4 Chino Hills earthquake—centered at a distance of 40 km—did not cause any observable damage, and reliable data were recorded. The acceleration records indicate that the peak acceleration of 2.6% g at the ground was amplified to 4.2% g at the roof. This data was used to compute vibration properties of the building by applying two system-identification techniques: the deterministic-stochastic-subspace (DSS) method (Van Overshee and De Morre 1996) and the peak-picking (PP) method. Remarkably close agreement between the calculated (from the computer model) and identified values of vibration periods and modes was achieved as demonstrated in Table 1 (where the periods identified by both methods are listed) and in Figure 4 (where the natural vibration modes identified by the DSS method are presented). As expected, the translational and torsional motions of the symmetric-plan building are uncoupled. In Figure 5, displacement time series calculated from the computer model and observed values during the Chino-Hills earthquake

Table 1. Natural periods of vibration obtained from peak-picking (PP) method, deterministic-stochastic subspace (DSS) method, and computer model.

Mode	Direction	Identified period (s)		Computer model period (s)
		PP method	DSS method	
1	Translational y	1.58	1.53	1.53
2	Translational x	1.46	–	1.46
3	Torsional	1.08	1.07	1.02
4	Translational y	0.55	0.49	0.54
5	Translational x	0.50	–	0.50
6	Torsional	0.38	0.36	0.36

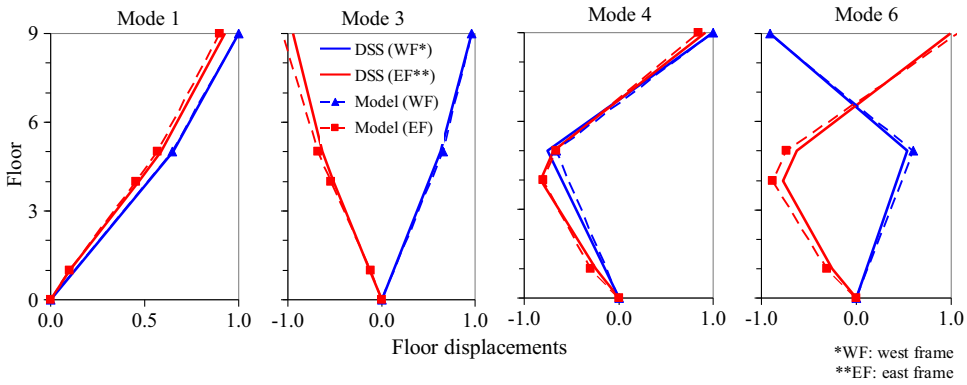

Figure 4. Comparison of natural vibration modes identified by the DSS method (red lines) with modes of the computer model (blue lines).

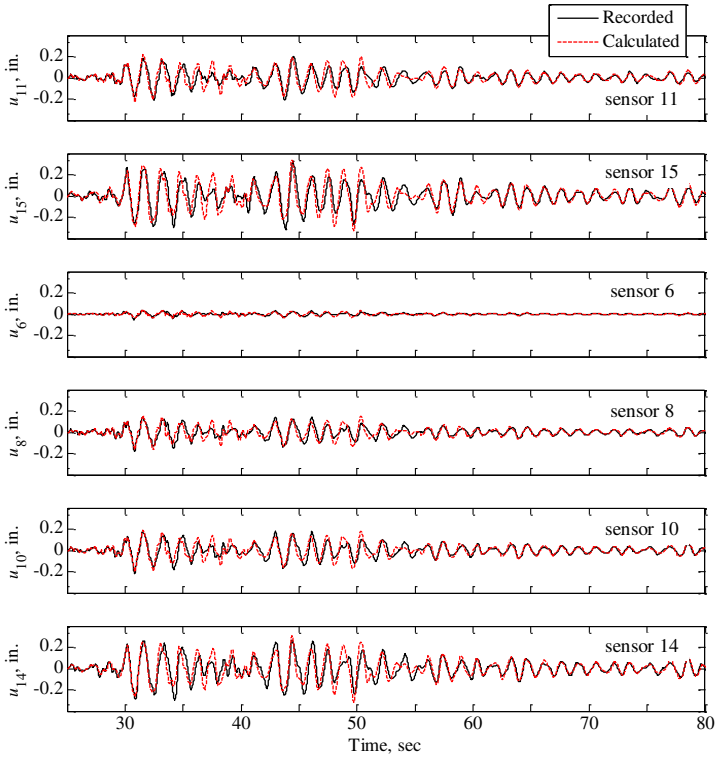

Figure 5. Comparison of recorded and computed floor displacements; recorded data is from the 2008 (M_w) 5.4 Chino Hills (Southern California) earthquake.

at various floors of the building are compared. An excellent match between the computed and observed response demonstrates the adequacy of the 3-D model.

The beams, columns, panel zones, and P-Δ effects of the asymmetric-plan building were modeled, as explained previously, for the symmetric-plan building, but the gravity columns were considered pinned at the base. In this system, the period of the dominantly torsional modes is longer than that of the dominantly lateral modes. Also, the higher-mode contributions to forces were expected to be significant because the effective mass of the first lateral mode is less than 50% of the total mass. Further details of both buildings are provided in Reyes and Kalkan (2012).

EVALUATION METHOD AND RESULTS

The following steps were implemented for evaluating the significance of the ground motion rotation angle on nonlinear behavior of buildings in near-fault sites.

1. For each of the 30 records selected for this investigation (see Table 1 in the companion paper for a list of those records), calculate the rotated ground-motion components by varying rotation angle θ_x from 0° to 360° at every 10° in the clockwise direction. The motions for $\theta_x = 0°$ and 90° correspond to the FP and FN components of the record, respectively. In addition, calculate the rotated ground-motion components for $\theta_x = \theta_m$ and $\theta_x = \theta_m + 90°$. For computing θ_m (maximum direction), use fundamental periods of the buildings. Definitions and illustrations of θ_x and θ_m are given in the companion paper.
2. Conduct linear and nonlinear RHAs of the two building models subjected to bi-directional rotated components of ground motions obtained in step 1. For each RHA, obtain story drifts (i.e., relative drift between two consecutive floors normalized by the story height), floor total accelerations at the center of mass, member chord rotations, and beam and column moments. This step involves 2,400 RHAs.

EDPs computed are the story drifts, floor total accelerations, member chord rotations, and beam and column moments at the first, third, fifth, seventh, and ninth floors of the buildings. Figure 6 plots the selected EDPs for the linear symmetric-plan building ($T_1 = 1.51$ s, where T_1 is the first-mode vibration period of the structure) as a function of the rotation angle θ_x subjected to ground motion no. 9, which has a maximum velocity-pulse period of 1.9 s. The filled gray area shows the values of θ_x, in which the velocity-pulses are identified according to the procedure by Baker (2007). The angles $\theta_x = 0°$ and 90° correspond to the fault-parallel and fault-normal directions, respectively. The record with a pulse period close to the fundamental period of the building is selected because such records impose sudden and intense energy demand associated with the velocity pulse that should be dissipated within a short period of time, which may cause large deformations in structures (Malhotra 1999, Bray and Rodriguez-Marek 2004; Kalkan and Kunnath 2006, 2007). The EDPs in this figure (and in similar polar plots shown later) are normalized to the maximum value of each EDP; actual values of EDPs are irrelevant hence they are not shown. Figure 6 indicates that maximum values of EDPs generally take place in the same direction, different than the FN direction (90°), with the exception of the ninth floor x-column moment. Also, the maximum EDPs are observed in the direction in which the velocity pulse is identified. For this particular record,

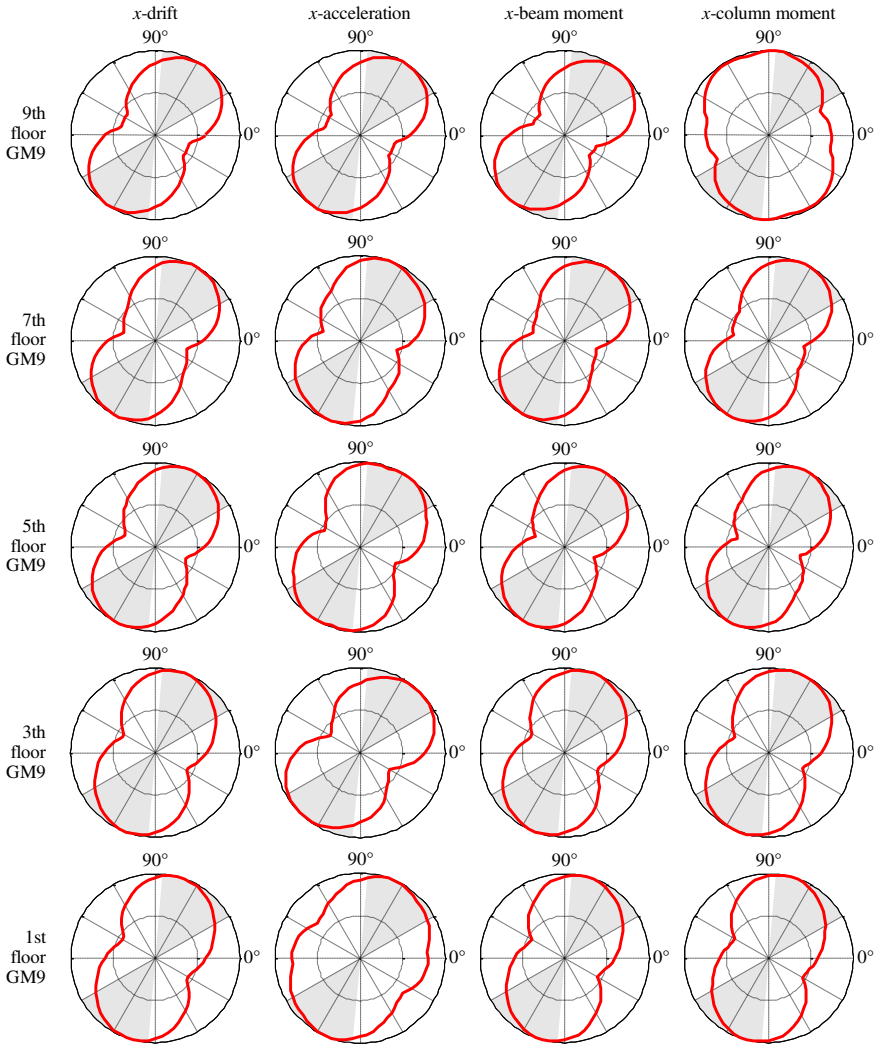

Figure 6. Normalized story drifts, floor total accelerations, and internal forces as a function of the rotation angle θ_x for the linear symmetric-plan building ($T_1 = 1.51$ s) subjected to ground motion (GM) no. 9, which has a maximum velocity-pulse period of 1.9 s close to the fundamental period of the building. The filled gray area shows values of θ_x in which the velocity-pulses are identified.

the FN direction does not contain an apparent velocity pulse, and the EDPs in the FN direction are 20% less than their maxima. Same response quantities are plotted in Figure 7 for the linear nine-story asymmetric-plan building ($T_1 = 2.5$ s) subjected to ground motion no. 2, which has a velocity-pulse period of 2.4 s. It is evident that θ_{cr}, defined as the angle corresponding to the largest response over all angles, varies significantly with the EDPs, and there is no optimum angle that leads to the peak values for all EDPs simultaneously.

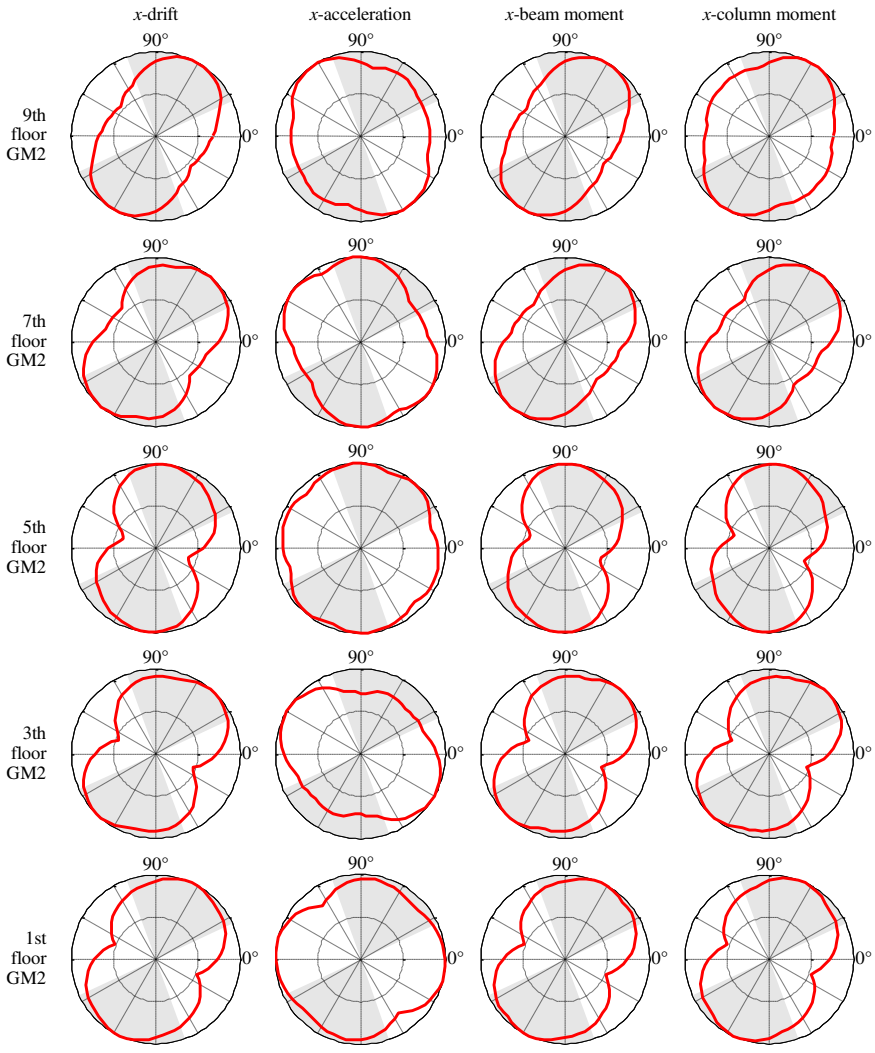

Figure 7. Normalized story drifts, floor total accelerations, and internal forces as a function of the rotation angle θ_x for the linear asymmetric-plan building ($T_1 = 2.5$ s) subjected to ground motion no. 2, which has a maximum velocity-pulse period of 2.4 s. The filled gray area shows values of θ_x in which the velocity pulses are identified.

For a given response quantity of interest and record pair, the FN/FP direction will correspond to two values; by comparing these two values with the responses at all other possible rotation angles, one can evaluate the level of conservatism in such directions or whether the MD or FN/FP directions' rotated ground motions provide an envelope of an EDP. If obvious systematic benefits of the MD or FN/FP orientations exist, they should be observable by repeating such comparisons for several EDPs and record pairs. To do this, the median values of EDPs and their dispersion are computed assuming

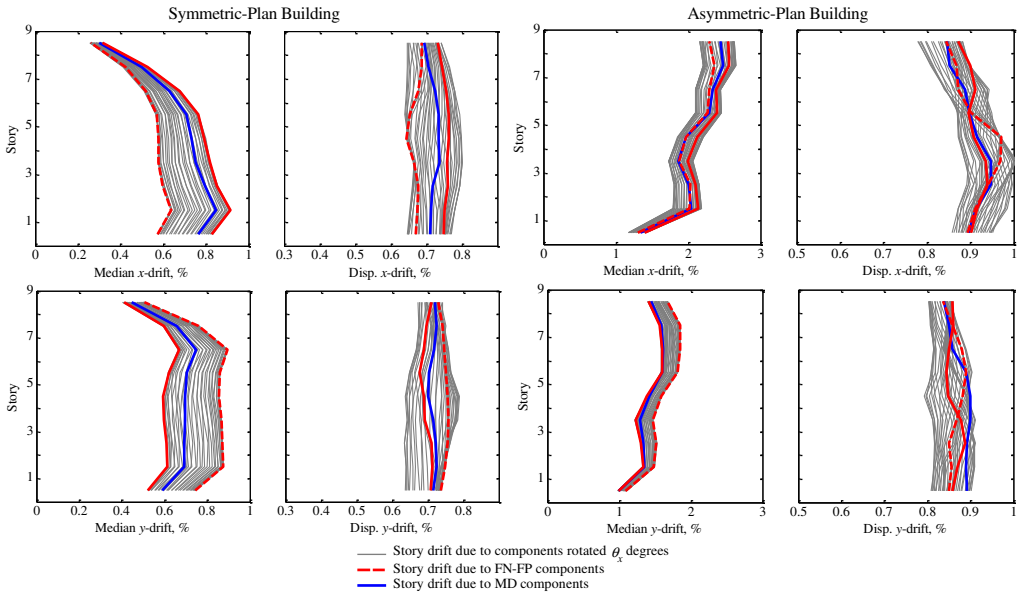

Figure 8. Height-wise distribution of median and dispersion (abbreviated as "Disp.") values of story drift in percent in the x and y directions for the linear symmetric- and asymmetric-plan buildings. The gray, red, and blue lines show median and dispersion of story drift due to 30 bi-directional ground motions in arbitrary orientations, in the FN/FP directions and in the maximum direction, respectively.

log-normal distribution. The median* value $\hat{x}$ and the dispersion measure σ of n observed values of x_i are calculated from:

$$\hat{x} = \exp\left[\frac{\sum_{i=1}^{n} \ln x_i}{n}\right]; \qquad \sigma = \left[\frac{\sum_{i=1}^{n} (\ln x_i - \ln \hat{x})}{n-1}\right]^{1/2} \tag{1}$$

Figure 8 shows the height-wise distribution of median and dispersion values of story drift plotted separately in x and y directions for linear response of the two buildings. In these plots, gray lines represent GMs rotated in 10° increments. The continuous red line is for the FN direction, and the dashed red line is for the FP direction. The blue line represents the ground-motion components oriented to the MD. Note that each line corresponds to either the median or dispersion of RHA results from 30 ground-motion pairs rotated by θ_x.

These figures present important findings. For the linear symmetric-plan system (left panels in Figure 8), the ground motions rotated to the FN direction yield the largest median EDPs in the x direction, whereas in the y direction, the motions oriented in the FP direction yield the largest median EDPs. Thus, EDPs due to the FN/FP-direction rotated ground motions serve as envelopes for all other non-redundant rotation angles. Note that the

*Geometric mean and the median are the same for log-normally distributed data.

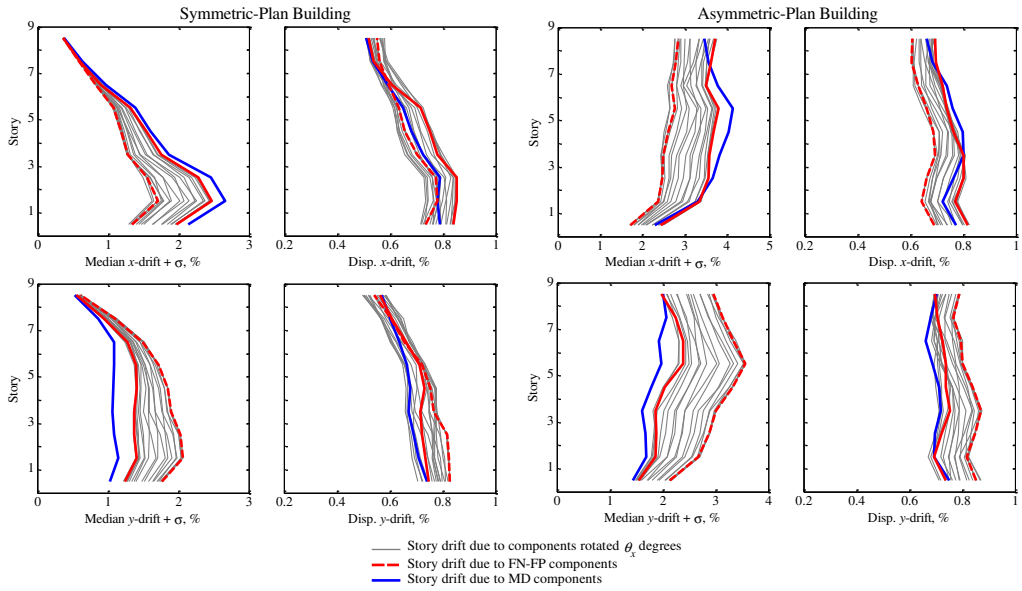

Figure 9. Height-wise distribution of median and dispersion (abbreviated as "Disp.") values of story drift in percent in the x and y directions for the nonlinear symmetric- and asymmetric-plan buildings. The gray, red, and blue lines show median + σ and dispersion of story drift due to 30 bi-directional ground motions in arbitrary orientations, in the FN/FP directions and in the maximum direction, respectively.

x direction (longitudinal direction of the building) coincides with 0° (FP direction). As opposed to the linear results based on single-story structures given in the companion paper, ground motions rotated to the MD produce smaller median EDPs than those due to FN/FP-direction rotated ground motions. Dispersions of EDPs are also larger in the FN/FP directions than in the MD. For the linear asymmetric-plan building (right panels in Figure 8), neither the FN/FP-direction nor the MD rotated ground motion produce the maximum median drift in the x direction. In the same direction, arbitrary orientations resulted in maximum median EDP values and the largest dispersion. However, in the y direction, ground motions rotated to FN/FP direction led to the maximum median drift. More importantly, the maximum median values of story drift in the x and y axes corresponded to the MD were smaller than those for the FN/FP direction, indicating that the ground motions rotated to the MD do not necessarily provide unrealistic EDPs as opposed to the critics in Stewart et al. (2011).

Figure 9 shows height-wise distribution of the median + $\sigma^{\dagger}$ and dispersion values of story drift plotted in percent separately in the x and y directions for the nonlinear responses of the two buildings. In this case, the ground motions rotated to the MD result in the maximum EDPs in the x direction, whereas the same records surprisingly produce the minimum EDPs in the y direction, in which the ground motions oriented to the FP direction yield

$^{\dagger}84^{th}$ percentile of EDPs are plotted to show significant nonlinear response.

175 the largest EDPs. Ground motions rotated to FN direction produce the second largest EDPs
176 following the results associated with the MD. Therefore, for nonlinear response, the MD- and
177 FP-direction rotated ground motions serve as envelopes for all other non-redundant rotation
178 angles. These records also yield the largest dispersion for both buildings. This observation is

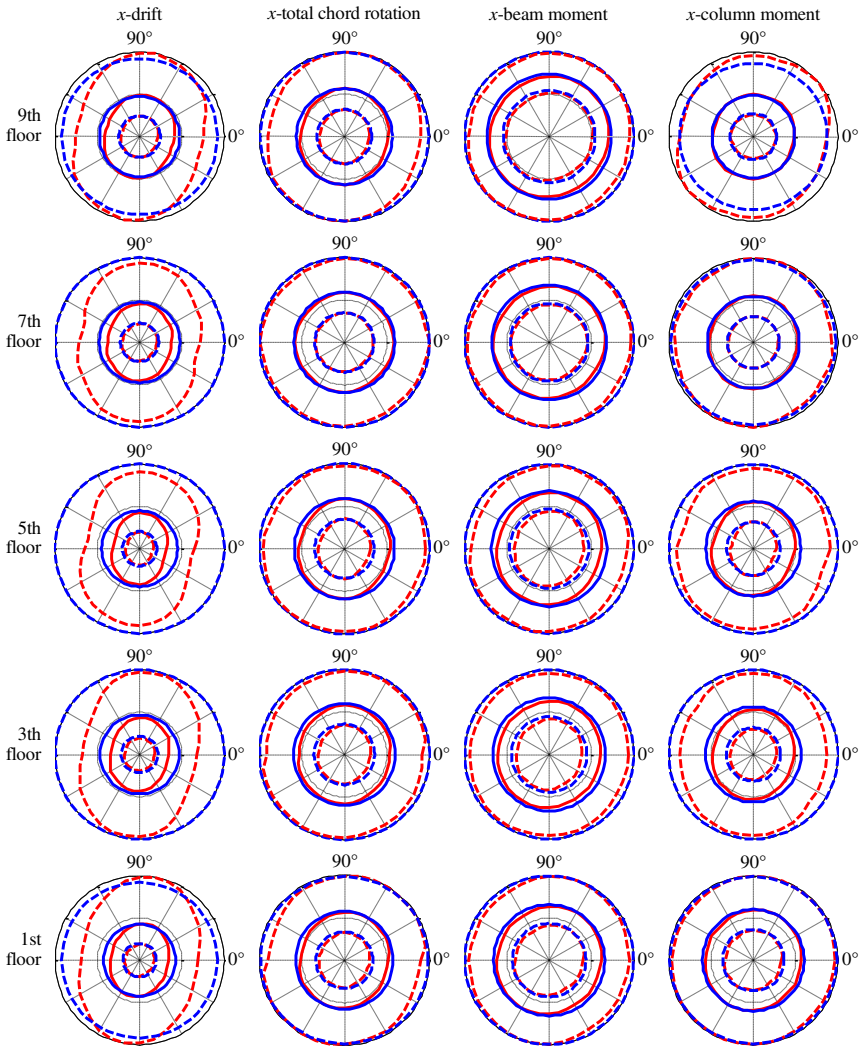

Figure 10. Median values of normalized story drifts at the corner, total chord rotations, and internal forces in the x direction as a function of the rotation angle, θ_x, for the nonlinear asymmetric-plan building subjected to 30 bi-directional ground motions. The red curves represent the median EDP values $\pm \sigma$. The blue circles represent the median-EDP values $\pm \sigma$ for the building subjected to bi-directional ground motions in the maximum–direction (MD). Note: Median EDP values are shown by solid curves, and 16^{th} and 84^{th} percentile EDP values are shown by dashed lines.

consistent for all EDPs investigated for both symmetric- and asymmetric-plan buildings as shown in Reyes and Kalkan (2012).

The nonlinear results plotted in Figure 9 (right panels) for story drift and other EDPs shown in Reyes and Kalkan (2012) are consolidated and depicted as a function of rotation

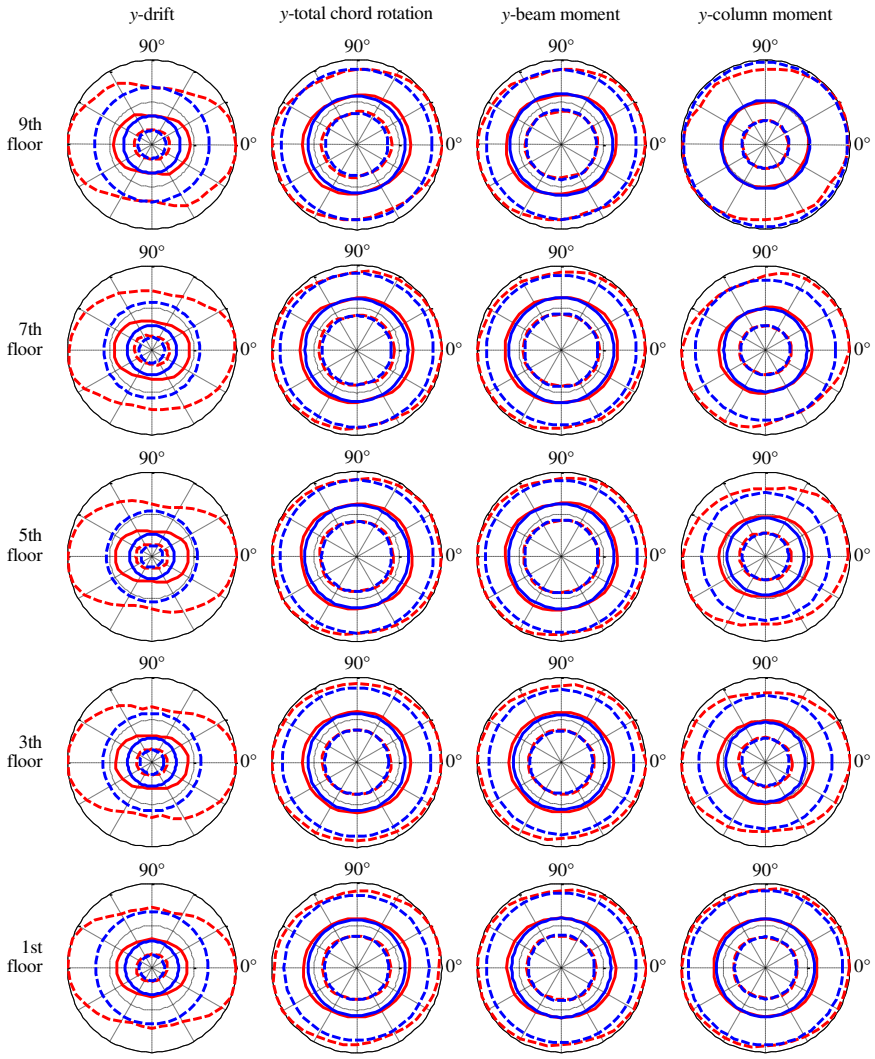

Figure 11. Median values of normalized story drifts, total chord rotations, and internal forces in the *y*-direction as a function of the rotation angle θ_x for the nonlinear nine-story asymmetric-plan building subjected to 30 bi-directional ground motions. The red curves represent the median EDP values $\pm \sigma$. The blue circles represent the median EDP values $\pm \sigma$ for the building subjected to bi-directional ground motions in the maximum–direction (MD). Note: Median EDP values are shown by solid curves, and 16^{th} and 84^{th} percentile EDP values are shown by dashed lines.

angle θ_x in Figure 10 and Figure 11 for x and y axes of the asymmetric-plan building, respectively. Viewing the response as a function of the rotation angle enables us to better understand how the critical angle θ_{cr} changes with both EDP and ground-motion pair. It is evident that θ_{cr} leading to the maximum response varies significantly with EDPs. While the FN/FP-direction rotated ground motions yield the largest value for certain EDPs, there is no single θ_{cr} that leads to the peak values for all EDPs simultaneously. Note that the same conclusion was drawn for linear single-story structures in the companion paper. These two figures prove that the maximum median EDPs (solid red line) are dependent on the rotation angle of the ground motion only for certain EDPs—for example member forces and plastic rotations are not affected by the rotation angle as much as story drift does. The maximum median EDPs due to the MD rotated ground motions yield conservative (either peak or close to peak) results only for the x direction of the building (Figure 10), whereas in the other direction, ground motions oriented to the FP direction provide the most conservative results (Figure 11). Thus, no consistency in over-conservatism of MD rotated ground motions is observed. Results for the symmetric-plan building are similar, therefore not repeated herein but available in Reyes and Kalkan (2012).

Next, median percent error in estimation of peak median response over all rotation angles due to MD- or FN/FP-direction rotated ground motions are computed using Equation 3 from the companion paper. The positive error means overestimation, and negative error means underestimation of peak median EDPs from 30 ground motion pairs. Using this equation, the error values are computed for nonlinear symmetric- and asymmetric-plan buildings and for EDPs shown in Figure 10 and Figure 11 along x and y axes; these results are presented in Table 2. The maximum value of underestimation and overestimation of peak median response when either MD- or FN/FP-direction rotated ground motions are used are 2% and 15%, respectively. For an individual ground motion pair, an underestimation of the

Table 2. Percent error in estimation of peak median response over all rotation angles using Equation 3 from the companion paper; positive error means overestimation, and negative error means underestimation (shown with bold numbers).

	x-direction				*y*-direction			
Structure	Drift	Chord rotation	Beam moment	Column moment	Drift	Chord rotation	Beam moment	Column moment
Symmetric-plan	5%	3%	0%	5%	**−1%**	**−2%**	**−2%**	**0%**
	8%	6%	3%	7%	**−1%**	**−2%**	**−1%**	**−1%**
	9%	6%	5%	9%	0%	**−1%**	**0%**	0%
	15%	11%	10%	6%	**−1%**	**−1%**	**−1%**	0%
	14%	11%	4%	2%	**0%**	**−1%**	**−1%**	**−1%**
Asymmetric-plan	**−1%**	0%	1%	**−2%**	0%	0%	**−1%**	**−1%**
	5%	0%	2%	**−1%**	**−1%**	0%	**0%**	**−1%**
	6%	0%	2%	1%	0%	**−1%**	**0%**	0%
	7%	3%	5%	5%	**−1%**	**0%**	0%	0%
	−1%	1%	1%	0%	**−1%**	**−2%**	0%	**−1%**

peak response may be up to 20% (see Figure 6 and Figure 7). These results indicate that conducting nonlinear RHA for a given ground-motion pair oriented in the MD or FN/FP directions does not always lead to the maximum EDPs overall orientations for systems responding in nonlinear range. However, if a suite of ground motion pairs rotated to MD and FN/FP directions is used for nonlinear RHAs, the median response will be very close or larger than the peak median response over all orientations. This important observation is true for both symmetric- and asymmetric-plan buildings.

CONCLUSIONS

The influence of the rotation angle of the ground motion on several engineering-demand parameters (EDPs) is systematically examined within a parametric study in the companion paper based on three-dimensional (3-D) computer models of single-story structures by varying their vibration period and response-modification factor R. In order to generalize the findings from these systems to multi-story structures, it is essential to perform further validation and verifications. For this purpose, 3-D linear and nonlinear computer models of nine-story buildings having symmetric (torsionally stiff) and asymmetric (torsionally flexible) layouts are subjected to a suite of bi-directional near-fault ground motions with and without apparent velocity-pulses. This investigation has led to the following conclusions:

- The rotation angle leading to the maximum-linear response is different than that leading to the maximum-nonlinear response; therefore, there is no single rotation angle that operates effectively in both linear and nonlinear range.
- The maximum story drift over all non-redundant orientations is in general polarized in the direction in which an apparent velocity-pulse with period close to fundamental period of the structure (T_1) is observed—this polarization is almost perfect for linear symmetric-plan building.
- Similar to the single-story structures, multi-story structures also show that there is no optimum orientation angle maximizing all EDPs simultaneously. The maximum value of an EDP can happen in any direction different than the direction of the apparent velocity-pulse.
- Conducting RHA for a ground motion oriented in the FN/FP or maximum direction (MD) does not always lead to the maximum EDPs' overall orientations for systems responding in nonlinear range; underestimation of the peak response may be up to 20%. This important observation is true for both symmetric- and asymmetric-plan buildings.
- The conclusions drawn above are for a given ground motion pair. The statistical evaluation of nonlinear single- and multi-story building models based on the large set of ground motion pairs suggest that, for practical applications in near-fault sites, RHAs should be conducted by rotating a set of records to the MD (computed at building's first-"mode" period) and FN/FP directions and by taking the maximum response values from these analyses as design values.
- We also recommend rotating ground motions to the MD and FN/FP directions for sites within 15 km of the fault instead of 5 km; the rationale for this recommendation is that propagating waves do not show notable attenuation within 15 km of the causative fault; thus, their intensity and frequency contents do not alter for events with high-seismic energy (moment magnitude >7.0).

ACKNOWLEDGMENTS

We wish to thank Katsuichiro Goda, two anonymous reviewers and responsible editor for their valuable comments and suggestions, which helped in improving the technical quality of the paper.

DATA AND RESOURCES

The earthquake data recorded from the nine-story instrumented building (CSMIP station no: 13364) is available at Center for Engineering Strong Motion Data (http://strongmotioncenter.org/).

REFERENCES

American Society of Civil Engineers (ASCE), 2010. *Minimum Design Loads for Buildings and Other Structures, ASCE/SEI 7-10*, Reston, VA.

American Society of Civil Engineers (ASCE), 2006. *Minimum Design Loads for Buildings and Other Structures, ASCE Standard 7-05*, Reston, VA.

American Society of Civil Engineers (ASCE), 2007. *Seismic Rehabilitation of Existing Buildings, Report No. 41–6*, Reston, VA.

Anagnostopoulos, S. A., Alexopoulou, C., and Stathopoulos, K. G., 2010. An answer to an important controversy and the need for caution when using simple models to predict inelastic earthquake response of buildings with torsion, *Earthquake Engng. Struct. Dyn.* **39**, 521–540.

Baker, J. W., 2007. Quantitative classification of near-fault ground motions using wavelet analysis, *Bulletin of the Seismological Society of America* **97**, 1486–1501.

Bray, J. D., and Rodriguez-Marek, A., 2004. Characterization of forward-directivity ground motions in the near-fault region, *Soil Dynamics and Earthquake Engineering* **24**, 815–828.

Computers and Structures, Inc. (CSI), 2006. *PERFORM-3D, User Guide v4, Nonlinear Analysis and Performance Assessment for 3-D Structures*, Computers and Structures, Inc., Berkeley, CA.

International Conference of Building Officials (ICBO), 2001. California Building Code, Whittier, CA.

International Conference of Building Officials (ICBO), 2009. International Building Code Whittier, CA.

International Conference of Building Officials (ICBO), 2010. California Building Code, Whittier, CA.

Kalkan, E., and Kunnath, S. K., 2006. Effects of fling-step and forward directivity on the seismic response of buildings, *Earthquake Spectra* **22**, 367–390.

Kalkan, E., and Kunnath, S. K., 2007. Effective cyclic energy as a measure of seismic demand, *Journal of Earthquake Engineering* **11**, 725–751.

Krawinkler, H., 1978. Shear in beam-column joints in seismic design of frames, *Engineering Journal* **15**, 82–91.

Malhotra, P. K., 1999. Response of buildings to near-field pulse-like ground motions, *Earthquake Engng. Struct. Dyn.* **28**, 1309–1326.

Reyes, J. C., and Chopra, A. K., 2012. Modal pushover-based scaling of two components of ground motion records for nonlinear RHA of structures, *Earthquake Spectra* **28**, 1243–1267.

294 Reyes, J. C., and Kalkan, E., 2012. *Should Ground motion Records be Rotated to Fault-Normal/*
295 *Parallel or Maximum-direction for Response History Analysis of Buildings*, U.S. Geological
296 Survey Open-File Report 2012-1261, 81 pp. (available at http://pubs.usgs.gov/of/2012/1261/).
297 Reyes, J. C., and Kalkan, E., 2015. Significance of rotating ground motions on behavior of
298 symmetric- and asymmetric-plan structures: part 1. single-story structures, *Earthquake*
299 *Spectra* **31**, xxx–xxx.
300 Stewart, J. P., Abrahamson, N. A., Atkinson, G. M., Baker, J., Boore, D. M., Bozorgnia, Y.,
301 Campbell, K. W., Comartin, C. D., Idriss, I. M., Lew, M., Mehrain, M., Moehle, J. P.,
302 Naeim, F., and Sabol, T. A., 2011. Representation of bi-directional ground motions for design
303 spectra in building codes. *Earthquake Spectra* **27**, 927–937.
304 Van Overschee, P., and De Moor, B., 1996. *Subspace Identification for Linear Systems*. Kluwer
305 Academic Publishers, Boston.

306 (Received 20 July 2012; accepted 18 September 2013)